

Mixed Convection from Vertical and Inclined Moving Sheets in a Parallel Freestream

N. Ramachandran,* T. S. Chen,† and B. F. Armaly‡

University of Missouri—Rolla, Rolla, Missouri

Laminar mixed convection adjacent to vertical and inclined moving sheets in a parallel freestream is analyzed for both the uniform wall temperature and the uniform surface heat flux cases. The analysis covers the entire mixed convection regime, from pure forced convection to pure free convection. Numerical results are reported for different combinations of the velocities of the moving sheet u_s and the freestream u_∞ for Prandtl numbers of 0.7 and 7. Local Nusselt numbers as well as velocity and temperature distributions are presented for a wide range of the buoyancy parameter. It is found that the local Nusselt number increases as the value of the buoyancy parameter increases. For the same dimensionless velocity difference $|U_s - U_\infty|$, the local Nusselt number is larger for $U_s > U_\infty$ than it is for $U_s < U_\infty$. Significant velocity overshoots occur within the boundary layer as the buoyancy parameter increases, with the low Prandtl number fluid exhibiting a more pronounced buoyancy effect than the high Prandtl number fluid. Simple correlations for evaluating local and average mixed convection Nusselt numbers are also presented and very good agreement is found between the computed results and the proposed simple correlations.

Nomenclature

C	= correlation constant
f, F	= reduced stream function for forced convection, = $\psi(x, y)/(v u_s x)^{1/2}$
f_1	= reduced stream function for free convection under uniform wall temperature (UWT), = $\psi(x, y)/[4\nu(Gr_x^* \cos \gamma/4)^{1/2}]$
F_1	= reduced stream function for free convection under uniform heat flux (UHF), = $\psi(x, y)/[5\nu(Gr_x^* \cos \gamma/5)^{1/2}]$
$G_1(Pr)$, $G_2(Pr)$, $G_3(Pr)$	= functions of Prandtl number defined, respectively, by Eqs. (39), (40), and (42)
$H_1(Pr)$, $H_2(Pr)$, $H_3(Pr)$	= functions of Prandtl number defined, respectively, by Eqs. (49), (50), and (52)
g	= gravitational acceleration
Gr_x	= local Grashof number for UWT, = $g\beta(T_w - T_\infty)x^3/\nu^2$
Gr_x^*	= local Grashof number for UHF, = $g\beta q_w x^4/k\nu^2$
Gr_L	= Grashof number based on L for UWT, = $g\beta(T_w - T_\infty)L^3/\nu^2$
Gr_L^*	= Grashof number based on L for UHF, = $g\beta q_w L^4/k\nu^2$
h, \bar{h}	= local and average heat-transfer coefficients
k	= thermal conductivity of fluid
L	= length of the plate
n	= constant exponent, Eqs. (32) and (33)
Nu_F, Nu_N , Nu_x	= local Nusselt numbers for pure forced, pure free, and mixed convection, = hx/k

$\overline{Nu}_F, \overline{Nu}_N$	= average Nusselt numbers
\overline{Nu}	for pure forced, pure free, and mixed convection, = $\bar{h}L/k$
Pr	= Prandtl number
q_w	= wall heat flux
Re_x	= local Reynolds number, = $u_s x/\nu$
Re_L	= Reynolds number based on L , = $u_s L/\nu$
T	= fluid temperature
T_w	= wall temperature
T_∞	= freestream temperature
u, v	= streamwise and normal velocity components
u_r	= reference velocity
u_s	= velocity of the moving sheet
u_∞	= freestream velocity
U_s	= normalized velocity of the moving surface
U_∞	= normalized freestream velocity
x, y	= axial and normal coordinates
Y_1	= dimensionless pseudosimilarity variable for free convection under UHF, = $(y/x)(Gr_x^* \cos \gamma/5)^{1/2}$
α	= thermal diffusivity
β	= volumetric coefficient of thermal expansion
γ	= angle of inclination from the vertical
δ	= boundary-layer thickness
ψ	= stream function
η	= dimensionless pseudosimilarity variable, forced convection, = $y(u_r/\nu x)^{1/2}$
η_1	= dimensionless pseudosimilarity variable for free convection under UWT, = $(y/x)(Gr_x \cos \gamma/4)^{1/2}$
ν	= kinematic viscosity of fluid
ρ	= density of fluid
θ, θ_1	= dimensionless temperature for UWT, = $(T - T_\infty)/(T_w - T_\infty)$
ϕ	= dimensionless temperature for forced convection under UHF, = $(T - T_\infty)Re_x^{1/2}/(q_w x/k)$
ϕ_1	= dimensionless temperature for free convection under UHF, = $(T - T_\infty)(Gr_x^* \cos \gamma/5)^{1/2}/(q_w x/k)$

Received April 18, 1986; revision received September 2, 1986.
Copyright © American Institute of Aeronautics and Astronautics,
Inc., 1987. All rights reserved.

*Graduate Research Assistant, Department of Mechanical and
Aerospace Engineering.

†Professor, Department of Mechanical and Aerospace Engineering.
Member AIAA.

‡Professor and Chairman, Department of Mechanical and Aero-
space Engineering. Member AIAA.

- ξ = buoyancy parameter for UWT,
 $= Gr_x \cos \gamma / Re_x^2$
 ξ_1 = forced flow parameter for UWT,
 $= (\frac{1}{2}) Re_x / (Gr_x \cos \gamma)^{\frac{1}{2}}$
 χ = buoyancy parameter for UHF,
 $= Gr_x^* \cos \gamma / Re_x^{\frac{5}{2}}$
 χ_1 = forced flow parameter for UHF,
 $= (\frac{1}{2}) Re_x / (Gr_x^* \cos \gamma / 5)^{\frac{5}{2}}$

Introduction

MIXED convection boundary-layer flows, characterized by the modification of the convective flow and thermal fields by buoyancy forces, are frequently encountered in transport processes occurring both in nature and in industry. To cite a few practical examples, industrial processes such as the extrusion of metals and plastics, cooling and/or drying of paper and textiles, and material handling involve boundary layers on continuous moving surfaces in a freestream under significant thermal buoyancy forces. The wall shear stress and the heat-transfer rate from the surface are affected by the buoyancy forces, and considerable error in their estimation (as high as 25%) can result if the buoyancy effects are not taken into account in the analysis.

At the outset, it must be pointed out that the problem of boundary-layer flow adjacent to a continuous moving sheet is physically different from that of the classical Blasius flow past a stationary flat plate and that the two problems cannot be mathematically transformed from one to the other. Sakiadis^{1,2} was the first to analyze the boundary layer on continuous semi-infinite sheets and cylindrical rods moving steadily in an otherwise quiescent environment. He examined the boundary-layer developments for these continuous surfaces. Several of the subsequent studies (see, for example, Moutsoglou and Chen³ and the references cited therein) dealt with the analysis of the boundary layer along moving fibers and sheets in a quiescent environment with and without the thermal buoyancy force effects on the flow. These studies have borne out the fact that thermal buoyancy forces significantly affect the flowfield and hence the heat-transfer rate from the surface, especially when the velocity of the moving surface is small and the temperature difference between the surface and the ambient fluid is large. Very recently, Abdelhazef⁴ analyzed the boundary layer along a moving surface maintained at uniform wall temperature (UWT) in a flowing parallel freestream. The relative velocity between the surface and the freestream governs the flowfield and hence the skin friction and the surface heat-transfer rate. However, in his study the effect of the thermal buoyancy forces on the flow and thermal fields was not considered and results were restricted to fluids with a Prandtl number of 0.7.

In the present study, the buoyancy force effects on the heat-transfer characteristics of laminar boundary layers along flat sheets moving in a parallel freestream (in the same direction of motion as the sheet) are examined analytically for the entire mixed convection regime, that is, from pure forced convection (no buoyancy forces) to pure free convection (fully buoyant flow). The sheet is maintained at a uniform wall temperature (UWT) or subjected to a uniform surface heat flux (UHF) and is moving parallel to the freestream in a vertical or inclined direction. Only the buoyancy-assisting case, which corresponds to the upward motion for a heated sheet or the downward motion for a cooled sheet, is investigated in this study. Results are reported for two Prandtl numbers of 0.7 and 7. Simple correlations for determining the local and average Nusselt numbers are also presented.

Analysis

Consider a semi-infinite flat sheet originating from a slot and moving at a constant velocity u_s in a vertical or inclined

direction in a parallel freestream with a constant velocity u_∞ as shown in Fig. 1. The stationary coordinate system has its origin located at the end of the slot, with the positive x coordinate extending in the streamwise direction and the y coordinate being measured normal to the surface. The normal coordinate y is taken to be positive away from the surface both for the fluid above and below the sheet. The inclination is measured as the acute angle from the vertical. The sheet may be maintained at a uniform wall temperature (UWT) or be subjected to a uniform surface heat flux (UHF). To investigate the entire range of mixed convection, ranging from pure forced convection to pure free convection, the analysis is carried out from both the standpoints of the buoyancy force effect on forced convection (i.e., forced-convection-dominated regime) and the forced flow effect on free convection (i.e., free-convection-dominated regime).

The governing boundary-layer equations with the Boussinesq approximation and the appropriate boundary conditions for the problem under consideration can be written as

$$\frac{\partial u}{\partial x} + \frac{\partial v}{\partial y} = 0 \quad (1)$$

$$u \frac{\partial u}{\partial x} + v \frac{\partial u}{\partial y} = \nu \frac{\partial^2 u}{\partial y^2} + g \beta \cos \gamma (T - T_\infty) \quad (2)$$

$$u \frac{\partial T}{\partial x} + v \frac{\partial T}{\partial y} = \alpha \frac{\partial^2 T}{\partial y^2} \quad (3)$$

$$u = u_s, v = 0, T = T_w \text{ or } q_w = -k \frac{\partial T}{\partial y} \text{ at } y = 0$$

$$u \rightarrow u_\infty, T \rightarrow T_\infty \text{ as } y \rightarrow \infty \quad (4)$$

In writing Eq. (2) the streamwise pressure gradient term induced by the buoyancy force is neglected. As was shown by Mucoglu and Chen,⁵ this approximation is valid when the condition

$$\frac{\delta}{x} \tan \gamma \ll 1 \text{ or } \tan \gamma \ll Re_x^{\frac{1}{2}} / \eta_\delta \quad (5)$$

is fulfilled, where $\eta_\delta = \delta(u_s/\nu x)^{\frac{1}{2}}$ and $Re_x = u_s x / \nu$. For laminar boundary layer with $10^3 \leq Re_x \leq 10^5$ and $5 \leq \eta_\delta \leq 10$, Eq. (5) yields γ values as high as 80 deg. Thus, Eq. (2) can be used with sufficient accuracy for inclined plates for angles γ up to 80 deg from the vertical.

Forced-Convection-Dominated Regime

To simplify the analysis, the velocities in Eqs. (1–3) and in the boundary conditions [Eq. (4)] are normalized by a reference velocity u_r , which is the larger of the two velocities u_s and u_∞ in the problem. Thus,

$$u_r = u_s \text{ for } u_s > u_\infty \text{ and } u_r = u_\infty \text{ for } u_s < u_\infty \quad (6)$$

$$U_s = u_s / u_r \text{ and } U_\infty = u_\infty / u_r \quad (7)$$

The governing equations and the boundary conditions are then transformed using the appropriate transformation variables for the UWT and UHF cases.

For the UWT case, the dimensionless stream function $f(\xi, \eta)$ and temperature $\theta(\xi, \eta)$ are introduced, respectively, as

$$f(\xi, \eta) = \frac{\psi(x, y)}{(\nu u_r x)^{\frac{1}{2}}}, \theta(\xi, \eta) = \frac{(T - T_\infty)}{(T_w - T_\infty)} \quad (8)$$

where the dimensional stream function $\psi(x, y)$ satisfies the continuity equation (1) with $u = \partial \psi / \partial y$ and $v = -\partial \psi / \partial x$. In

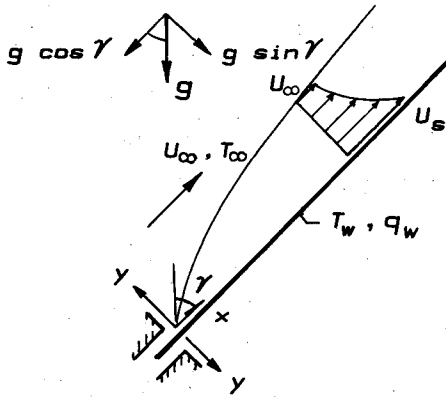


Fig. 1 A schematic of flow configuration.

terms of the transformation coordinates (ξ, η) defined as

$$\xi = Gr_x \cos \gamma / Re_x^2, \quad \eta = y(u_r/\nu x)^{1/2} \quad (9)$$

Eqs. (1-4) can be transformed into the following system of equations:

$$f''' + \frac{1}{2}ff'' + \xi\theta = \xi \left(f' \frac{\partial f'}{\partial \xi} - f'' \frac{\partial f}{\partial \xi} \right) \quad (10)$$

$$\frac{1}{Pr}\theta'' + \frac{1}{2}f\theta' = \xi \left(f' \frac{\partial \theta}{\partial \xi} - \theta' \frac{\partial f}{\partial \xi} \right) \quad (11)$$

$$\begin{aligned} f'(\xi, 0) &= u_s/u_r, \quad f(\xi, 0) = 0, \quad \theta(\xi, 0) = 1 \\ f'(\xi, \infty) &= u_\infty/u_r, \quad \theta(\xi, \infty) = 0 \end{aligned} \quad (12)$$

where the primes denote partial derivatives with respect to η .

In a similar manner, the system of equations for the UHF case can be derived. These equations are given in Chen et al.⁶ and are thus omitted here. However, the corresponding boundary conditions are changed to

$$\begin{aligned} F'(\chi, 0) &= u_s/u_r, \quad F(\chi, 0) = 0, \quad \phi'(\chi, 0) = -1 \\ F'(\chi, \infty) &= u_\infty/u_r, \quad \phi(\chi, \infty) = 0 \end{aligned} \quad (13)$$

where the primes again denote partial differentiations with respect to η , $F(\chi, \eta)$ is the reduced stream function, and $\phi(\chi, \eta)$ is the dimensionless temperature. The buoyancy parameter for this case is defined as

$$\chi = Gr_x^* \cos \gamma / Re_x^2 \quad (14)$$

The local and average Nusselt numbers for the UWT case have the respective expressions

$$Nu_x Re_x^{-1/2} = -\theta'(\xi, 0) \quad (15)$$

and

$$\overline{Nu} Re_L^{-1/2} = \xi_L^{-1/2} \int_0^{\xi_L} \xi^{-1/2} [-\theta'(\xi, 0)] d\xi \quad (16)$$

For the UHF case, they are given by

$$Nu_x Re_x^{-1/2} = 1/\phi(\chi, 0) \quad (17)$$

$$\overline{Nu} Re_L^{-1/2} = \frac{2}{3} \chi_L^{-1/2} \int_0^{\chi_L} \chi^{-1/2} [1/\phi(\chi, 0)] d\chi \quad (18)$$

In the above equations, ξ_L , χ_L , and Re_L , are, respectively, the ξ , χ , and Re_x based on a certain sheet length L in the flow direction.

The system of equations along with relevant boundary conditions for the forced-convection-dominated regime are solved by an accurate and efficient finite-difference scheme similar to the one used by Keller and Cebeci.^{7,8} Numerical results were obtained for five different velocity combinations (U_s, U_∞) of (1,1), (1,0.5), (1,0), (0.5,1) and (0,1) for both $Pr = 0.7$ and 7, covering the respective buoyancy parameter ranges of $0 \leq \xi \leq 10$ and $0 \leq \chi \leq 10$ for the UWT and UHF cases. As is evident, the (0,1) velocity combination corresponds to flow along a stationary vertical or inclined surface and the (1,0) velocity combination to a surface moving in an otherwise quiescent environment. Also, $\xi = 0$ and $\chi = 0$ correspond to pure forced convection, respectively, for the UWT and UHF cases.

Free-Convection-Dominated Regime

For the free-convection-dominated regime, the transformed equations and boundary conditions for the UWT case under Eq. (5) are given by

$$f_1''' + 3f_1f_1'' - 2f_1'^2 + \theta_1 = 2\xi_1 \left(f_1'' \frac{\partial f_1}{\partial \xi_1} - f_1' \frac{\partial f_1'}{\partial \xi_1} \right) \quad (19)$$

$$\frac{1}{Pr}\theta_1'' + 3f_1\theta_1' = 2\xi_1 \left(\theta_1' \frac{\partial f_1}{\partial \xi_1} - f_1' \frac{\partial \theta_1}{\partial \xi_1} \right) \quad (20)$$

$$\begin{aligned} f_1'(\xi_1, 0) &= \xi_1, \quad f_1(\xi_1, 0) = 0, \quad \theta_1(\xi_1, 0) = 1 \\ f_1'(\xi_1, \infty) &= \xi_1 U_\infty, \quad \theta_1(\xi_1, \infty) = 0 \end{aligned} \quad \text{for } U_s > U_\infty \quad (21)$$

and

$$\begin{aligned} f_1'(\xi_1, 0) &= \xi_1 U_s, \quad f_1(\xi_1, 0) = 0, \quad \theta_1(\xi_1, 0) = 1 \\ f_1'(\xi_1, \infty) &= \xi_1, \quad \theta_1(\xi_1, \infty) = 0 \end{aligned} \quad \text{for } U_s < U_\infty \quad (22)$$

where the dimensionless stream function $f_1(\xi_1, \eta_1)$ and the dimensionless temperature $\theta_1(\xi_1, \eta_1)$, are now defined as

$$f_1(\xi_1, \eta_1) = \frac{\psi(x, y)}{4\nu(Gr_x \cos \gamma/4)^{1/4}} \quad (23a)$$

$$\theta_1(\xi_1, \eta_1) = \frac{(T - T_\infty)}{(T_w - T_\infty)} \quad (23b)$$

The primes in the above equations denote partial differentiation with respect to η_1 and the forced flow parameter ξ_1 is given by

$$\xi_1 = \frac{1}{2} Re_x / (Gr_x \cos \gamma)^{1/2} = \frac{1}{2} \xi^{-1/2} \quad (24)$$

The local and average Nusselt numbers for this case are given by

$$Nu_x (Gr_x \cos \gamma/4)^{-1/4} = -\theta_1'(\xi_1, 0) \quad (25)$$

and

$$\overline{Nu} (Gr_L \cos \gamma/4)^{-1/4} = -2\xi_{1L}^{1/2} \int_0^{\xi_{1L}} \xi_1^{-1/2} [-\theta_1'(\xi_1, 0)] d\xi_1 \quad (26)$$

where $\xi_{1L} = \xi_1(L)$.

For the UHF case, the transformed $F_1(\chi_1, Y_1)$ and $\phi_1(\chi_1, Y_1)$ equations are given in Chen et al.⁶ and are not

repeated here. The boundary conditions, however, must be changed to

$$\begin{aligned} F_1'(\chi_1, 0) &= \chi_1, & F_1(\chi_1, 0) &= 0, & \phi_1'(\chi_1, 0) &= -1 \\ F_1'(\chi_1, \infty) &= \chi_1 U_\infty, & \phi_1(\chi_1, \infty) &= 0 \\ & \text{for } U_s > U_\infty \end{aligned} \quad (27)$$

and

$$\begin{aligned} F_1'(\chi_1, 0) &= \chi_1 U_s, & F_1(\chi_1, 0) &= 0, & \phi_1'(\chi_1, 0) &= -1 \\ F_1'(\chi_1, \infty) &= \chi_1, & \phi_1(\chi_1, \infty) &= 0 \\ & \text{for } U_s < U_\infty \end{aligned} \quad (28)$$

where the primes now denote partial differentiations with respect to Y_1 and the forced flow parameter χ_1 is given by

$$\chi_1 = \frac{1}{5} \frac{Re_x}{(Gr_x^* \cos \gamma / 5)^{\frac{2}{5}}} = (5^3 \chi^2)^{-\frac{1}{5}} \quad (29)$$

The local and average Nusselt numbers now have the expressions

$$Nu_x (Gr_x^* \cos \gamma / 5)^{-\frac{1}{5}} = 1 / \phi_1(\chi_1, 0) \quad (30)$$

and

$$\overline{Nu} \left(\frac{Gr_L^* \cos \gamma}{5} \right)^{-\frac{1}{5}} = -\frac{5}{3} \chi_{1L}^{\frac{4}{5}} \int_0^{\chi_{1L}} \chi_1^{-\frac{7}{5}} [1 / \phi_1(\chi_1, 0)] d\chi_1 \quad (31)$$

where $\chi_{1L} = \chi_1(L)$.

The system of equations along with relevant boundary conditions for the free-convection-dominated regime are solved by the local nonsimilarity method, with the equations being truncated at the second level. Solutions were obtained for five different velocity combinations (U_s, U_∞) of (1, 1), (1, 0.5), (1, 0), (0.5, 1), and (0, 1) in the buoyancy parameter ranges of $10 \leq \xi_1 \leq \infty$ and $10 \leq \chi_1 \leq \infty$ for both $Pr = 0.7$ and 7. The upper limit ∞ in these ranges corresponds to pure free convection for the UWT and UHF cases, respectively. The solutions obtained from both ends (the pure forced convection end and the pure free convection end) were matched with errors of less than 4% at the corresponding buoyancy parameter value of 10.

Correlations

Correlations for the local mixed convection Nusselt numbers are proposed along the same line as suggested for mixed convection from stationary isothermal inclined surfaces by Chen et al.⁹ for the UWT condition and by Armaly et al.¹⁰ for the UHF condition. Accordingly, the local mixed convection Nusselt number Nu_x can be expressed in terms of the local Nusselt number for pure forced convection from continuous moving sheets Nu_F and the local Nusselt number for pure free convection Nu_N for the same geometry as

$$Nu_x^n = Nu_F^n + Nu_N^n \quad (32)$$

where n is a constant exponent. Equation (32) can be readily cast into the following form

$$Y^n = 1 + X^n \quad (33)$$

where

$$Y = Nu_x / Nu_F, \quad X = Nu_N / Nu_F \quad (34)$$

The average Nusselt number \overline{Nu} can also be obtained from Eqs. (32) and (33) if the respective local Nusselt numbers

Nu_x , Nu_F , and Nu_N are replaced with the corresponding average quantities \overline{Nu} , \overline{Nu}_F , and \overline{Nu}_N . The expressions used in the correlation of Eq. (32) are presented below for both the UWT and the UHF cases.

Uniform Wall Temperature (UWT) Case

The local Nusselt number for the pure forced convection in laminar boundary layer along continuous moving isothermal sheets exposed to a parallel freestream can be expressed with good accuracy of less than 2% error as follows:

$$Nu_F = (CPr)^m G_1(Pr) Re_x^{\frac{1}{2}}, \quad U_s > U_\infty \quad (35)$$

$$Nu_F = (CPr)^m G_2(Pr) Re_x^{\frac{1}{2}}, \quad U_s < U_\infty \quad (36)$$

where C and m are constants. The values for C are listed in Table 1. The constant m is defined as

$$m = U_\infty / (U_s + U_\infty), \quad U_s > U_\infty \quad (37)$$

$$m = U_s / (U_s + U_\infty), \quad U_s < U_\infty \quad (38)$$

The function $G_1(Pr)$ is given by Ramachandran et al.¹¹ to correlate the pure forced convection Nusselt number for vertical and inclined isothermal sheets moving in an otherwise quiescent environment, that is, for the case $m = 0$ in Eq. (35). The other function $G_2(Pr)$ has been given by Churchill and Ozoe¹² for correlating the pure forced convection Nusselt number over an isothermal stationary flat plate, that is, for the case $m = 0$ in Eq. (36). The respective expressions for $G_1(Pr)$ and $G_2(Pr)$ are

$$G_1(Pr) = -1.44472 Pr^{\frac{1}{5}} + 1.8865 Pr^{\frac{13}{32}} \quad (39)$$

and

$$G_2(Pr) = 0.339 Pr^{\frac{1}{3}} \left[1 + (0.0468 / Pr)^{\frac{2}{3}} \right]^{-\frac{1}{4}} \quad (40)$$

The corresponding local Nusselt number expression for free convection can be given by a modified form of Ede¹³ as

$$Nu_N = G_3(Pr) (Gr_x \cos \gamma)^{\frac{1}{4}} \quad (41)$$

Table 1 Correlation constants and regime of mixed convection

Case ^a	Pr	C	Flow condition	U_s	U_∞	a	b
UWT	0.7	2.55	$U_s > U_\infty$	1	1	0.45	60
				1	0.5	0.25	40
				1	0	0.09	30
			$U_s < U_\infty$	0.5	1	0.20	25
				0	1	0.07	7.5
				0	0	0.00	0
	7	0.16	$U_s > U_\infty$	1	1	1.50	350
				1	0.5	0.70	300
				1	0	0.30	250
			$U_s < U_\infty$	0.5	1	0.40	100
				0	1	0.10	8.5
				0	0	0.00	0
UHF	0.7	2.10	$U_s > U_\infty$	1	1	2.00	250
				1	0.5	1.50	150
				1	0	1.25	100
			$U_s < U_\infty$	0.5	1	0.70	80
				0	1	0.04	20
				0	0	0.00	0
	7	0.15	$U_s > U_\infty$	1	1	25.00	5000
				1	0.5	20.00	4500
				1	0	10.00	4000
			$U_s < U_\infty$	0.5	1	4.00	1500
				0	1	0.15	22
				0	0	0.00	0

^aUWT: $a \leq \xi \leq b$. UHF: $a \leq \chi \leq b$.

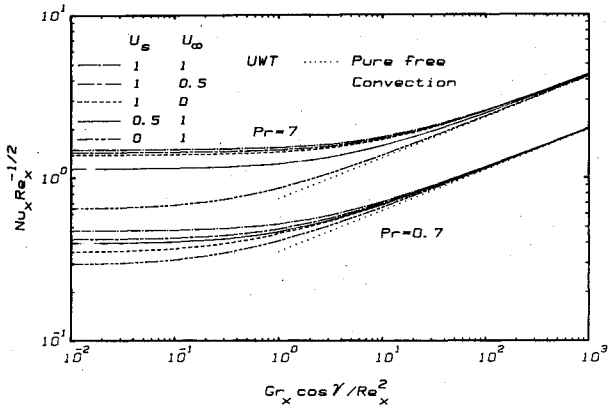


Fig. 2 Local Nusselt number results for inclined isothermal moving sheets.

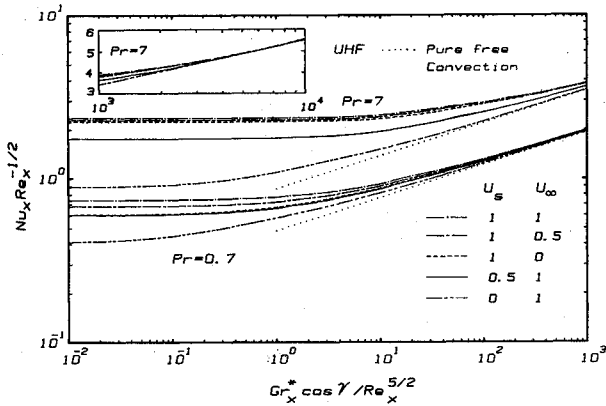


Fig. 3 Local Nusselt number results for inclined moving sheets with uniform surface heat flux.

where

$$G_3(Pr) = 0.75 Pr^{1/2} [2.5(1 + 2Pr^{1/2} + 2Pr)]^{-1/4} \quad (42)$$

Pure free convection corresponds to the case when both $U_s = 0$ and $U_\infty = 0$ simultaneously.

The local mixed convection Nusselt number can then be expressed according to Eq. (33) as follows:

$$\frac{Nu_x Re_x^{-1/2}}{G_1(Pr)} = \left\{ 1 + \left[\frac{G_3(Pr)(Gr_x \cos \gamma / Re_x^2)^{1/4}}{(CPr)^m G_1(Pr)} \right]^n \right\}^{1/n} \quad \text{for } U_s > U_\infty \quad (43)$$

and

$$\frac{Nu_x Re_x^{-1/2}}{G_2(Pr)} = \left\{ 1 + \left[\frac{G_3(Pr)(Gr_x \cos \gamma / Re_x^2)^{1/4}}{(CPr)^m G_2(Pr)} \right]^n \right\}^{1/n} \quad \text{for } U_s < U_\infty \quad (44)$$

Similarly, the average mixed convection Nusselt number can be correlated as

$$\frac{\overline{Nu} Re_L^{-1/2}}{2G_1(Pr)} = \left\{ 1 + \left[\frac{2G_3(Pr)(Gr_L \cos \gamma / Re_L^2)^{1/4}}{3(CPr)^m G_1(Pr)} \right]^n \right\}^{1/n} \quad \text{for } U_s > U_\infty \quad (45)$$

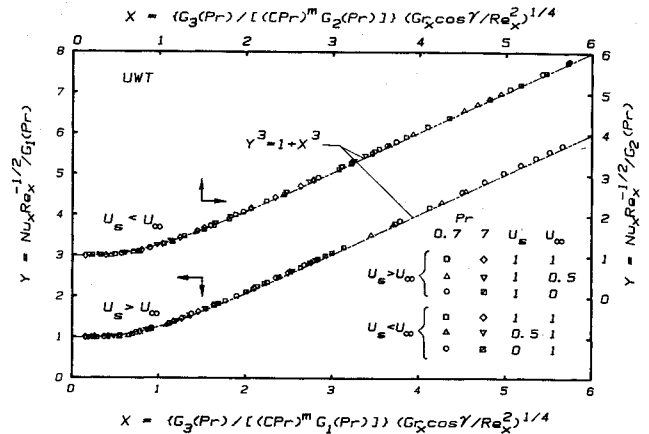


Fig. 4 Comparison between predicted and correlated local Nusselt numbers for inclined isothermal moving sheets.

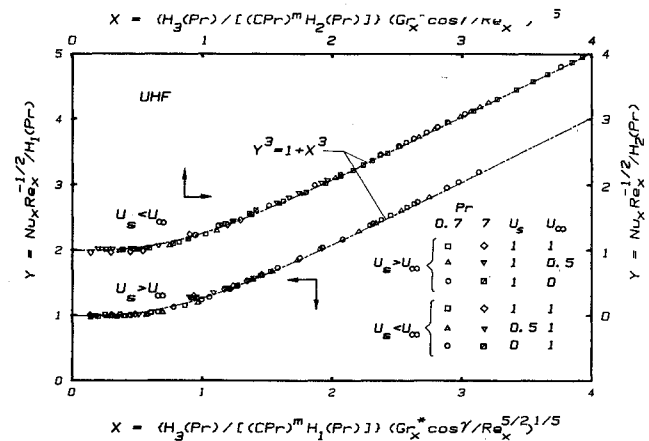


Fig. 5 Comparison between predicted and correlated local Nusselt numbers for inclined moving sheets with uniform surface heat flux.

and

$$\frac{\overline{Nu} Re_L^{-1/2}}{2G_2(Pr)} = \left\{ 1 + \left[\frac{2G_3(Pr)(Gr_L \cos \gamma / Re_L^2)^{1/4}}{3(CPr)^m G_2(Pr)} \right]^n \right\}^{1/n} \quad \text{for } U_s < U_\infty \quad (46)$$

Equations (43–46) have the form $Y = (1 + X^n)^{1/n}$. For a vertical plate, $\gamma = 0$ deg and $\cos \gamma = 1$.

Uniform Surface Heat Flux (UHF) Case

As in the UWT case, the local Nusselt number for pure forced convection in a laminar layer along moving sheets subjected to the UHF condition and exposed to a parallel freestream can be accurately expressed (to within 2% error) as

$$Nu_F = (CPr)^m H_1(Pr) Re_x^{1/2}, \quad U_s > U_\infty \quad (47)$$

$$Nu_F = (CPr)^m H_2(Pr) Re_x^{1/2}, \quad U_s < U_\infty \quad (48)$$

where C is a constant whose values are listed in Table 1 and m is given as before by Eqs. (37) and (38). The function $H_1(Pr)$ corresponds to the correlation for pure forced convection Nusselt numbers for vertical and inclined sheets subjected to a uniform surface heat flux and moving in a stationary medium.¹¹ The function $H_2(Pr)$ has been given by Churchill and Ozoe¹² for correlating pure forced convection Nusselt numbers over a stationary flat plate with the UHF

condition. The expressions for $H_1(Pr)$ and $H_2(Pr)$ are, respectively,

$$H_1(Pr) = -2.09467Pr^{\frac{1}{3}} + 2.8452Pr^{\frac{13}{32}} \quad (49)$$

and

$$H_2(Pr) = 0.464Pr^{\frac{1}{3}} \left[1 + (0.0207/Pr)^{\frac{1}{3}} \right]^{-\frac{1}{4}} \quad (50)$$

The corresponding local Nusselt number expression for free convection can be given by¹⁴

$$Nu_N = H_3(Pr)(Gr_x^* \cos \gamma)^{\frac{1}{5}} \quad (51)$$

where

$$H_3(Pr) = Pr^{\frac{2}{3}} [4 + 9Pr^{\frac{1}{3}} + 10Pr]^{-\frac{1}{5}} \quad (52)$$

The local mixed convection Nusselt number can then be expressed as before by Eq. (33) as follows:

$$\begin{aligned} & \frac{Nu_x Re_x^{-\frac{1}{2}}}{H_1(Pr)} \\ &= \left\{ 1 + \left[\frac{H_3(Pr)(Gr_x^* \cos \gamma / Re_x^{\frac{5}{2}})^{\frac{1}{5}}}{(CPr)^m H_1(Pr)} \right]^n \right\}^{1/n} \quad \text{for } U_s > U_\infty \end{aligned} \quad (53)$$

$$\begin{aligned} & \frac{Nu_x Re_x^{-\frac{1}{2}}}{H_2(Pr)} \\ &= \left\{ 1 + \left[\frac{H_3(Pr)(Gr_x^* \cos \gamma / Re_x^{\frac{5}{2}})^{\frac{1}{5}}}{(CPr)^m H_2(Pr)} \right]^n \right\}^{1/n} \quad \text{for } U_s < U_\infty \end{aligned} \quad (54)$$

Similarly, the average mixed convection Nusselt number can be correlated as

$$\begin{aligned} & \frac{\overline{Nu} Re_L^{-\frac{1}{2}}}{2H_1(Pr)} \\ &= \left\{ 1 + \left[\frac{5H_3(Pr)(Gr_L^* \cos \gamma / Re_L^{\frac{5}{2}})^{\frac{1}{5}}}{8(CPr)^m H_1(Pr)} \right]^n \right\}^{1/n} \quad \text{for } U_s > U_\infty \end{aligned} \quad (55)$$

and

$$\begin{aligned} & \frac{\overline{Nu} Re_L^{-\frac{1}{2}}}{2H_2(Pr)} \\ &= \left\{ 1 + \left[\frac{5H_3(Pr)(Gr_L^* \cos \gamma / Re_L^{\frac{5}{2}})^{\frac{1}{5}}}{8(CPr)^m H_2(Pr)} \right]^n \right\}^{1/n} \quad \text{for } U_s < U_\infty \end{aligned} \quad (56)$$

Again, Eqs. (53–56) have the form $Y = (1 + X^n)^{1/n}$.

Results and Discussion

The local mixed convection Nusselt numbers $Nu_x Re_x^{-\frac{1}{2}}$ as a function of the buoyancy parameter $Gr_x^* \cos \gamma / Re_x^2$ for the UWT case are illustrated in Fig. 2. Results are presented for the entire range of values of the buoyancy parameter for two Prandtl numbers, $Pr = 0.7$ and 7 , and for five different veloc-

ity combinations of moving sheet and freestream. Similar results for the UHF case are shown in Fig. 3, with the buoyancy parameter now being $Gr_x^* \cos \gamma / Re_x^2$. The results presented in both figures apply to a vertical moving sheet for $\gamma = 0$ deg and can be used with good accuracy for inclined moving sheets in the angle range of $0 \leq \gamma \leq 80$ deg from the vertical. From Figs. 2 and 3, it is evident that the pure forced convection local Nusselt number changes as the freestream velocity combination (U_s, U_∞) changes. Also, the local Nusselt number increases as the value of the buoyancy parameter increases and all the curves for the different (U_s, U_∞) combinations approach a common pure free convection asymptote (also shown in the figures). These figures also reveal that, for the same dimensionless velocity difference $|U_s - U_\infty|$, the local Nusselt number is larger for $U_s > U_\infty$ than it is for $U_s < U_\infty$. This trend, which was also observed in the results of Abdelhafez⁴ for pure forced convection, extends throughout the mixed convection regime. This increase in the surface heat-transfer rate can be attributed to a larger velocity and hence a higher transport rate in the vicinity of the sheet in the former case in comparison to the latter case. It is also of interest to note from Figs. 2 and 3 that the deviation of the local Nusselt number from the pure forced convection asymptote is more pronounced for the lower Prandtl number fluid ($Pr = 0.7$) than for the higher Prandtl number fluid ($Pr = 7$). The approach of the local Nusselt numbers to the pure free convection asymptotic value is thus delayed to higher values of the buoyancy parameter for the high Prandtl number fluids.

The predicted heat-transfer results from the analysis are compared with the proposed local Nusselt number correlations in Figs. 4 and 5 for the UWT and the UHF cases, respectively. The results are presented in terms of Y vs X in the figures. Thus, for the UWT case the results are cast into the form of Eqs. (43) and (44) and for the UHF case into the form of Eqs. (53) and (54). The correlated results are presented for both Prandtl numbers of $Pr = 0.7$ and 7 . As is evident from these two figures, an exponent value of $n = 3$ in Eq. (33) correlates very well with the numerically predicted mixed convection results from Eqs. (15), (17), (25), and (30). The agreement between the predicted and the correlated results for the UWT case (Fig. 4) is better (with errors of less than 5%) than that for the UHF case (with errors of less than 8%). Figures 4 and 5 also apply to average Nusselt number if the X and Y coordinates in the respective figures are replaced with the corresponding ones given in Eqs. (45) and (46) for Fig. 4 and in Eqs. (55) and (56) for Fig. 5. It should be noted that in applying the correlation equations to inclined plates, the inclination angle γ should be limited to 80 deg.

The effects of buoyancy force on the heat-transfer characteristics are presented in a different form in Fig. 6 for the UWT case. The predicted local Nusselt number $Nu_x Re_x^{-\frac{1}{2}}$ is plotted against the dimensionless velocity difference $|U_s - U_\infty|$ for four representative values of the buoyancy parameter (0, 1, 5, and 10) for both Prandtl numbers. Also presented in this figure are the proposed correlations that cover $0 \leq |U_s - U_\infty| \leq 1$. The following inferences can be drawn from Fig. 6:

1) There is a very good agreement between the proposed correlations and the numerically predicted results.

2) For the same dimensionless velocity difference $|U_s - U_\infty|$, the local Nusselt number is higher when $U_s > U_\infty$ than when $U_s < U_\infty$. This effect is more pronounced for a Prandtl number of 7 than for 0.7. Also, the difference in Nusselt numbers decreases as the value of buoyancy parameter increases.

3) As the buoyancy force increases, the local Nusselt number increases, with the low Prandtl number fluid exhibiting a higher relative increase in the Nusselt number than the high Prandtl number fluid for the same increase in the buoyancy force.

Representative velocity and temperature distributions for the UWT case are presented in Figs. 7–10 for the velocity

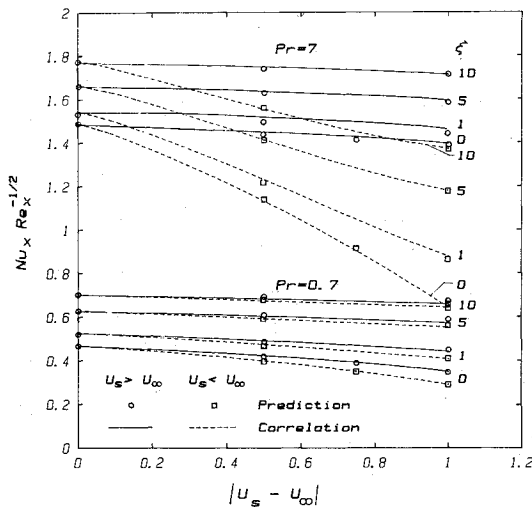


Fig. 6 Variations of the local Nusselt number with $|U_s - U_\infty|$ and the buoyancy parameter, UWT case.

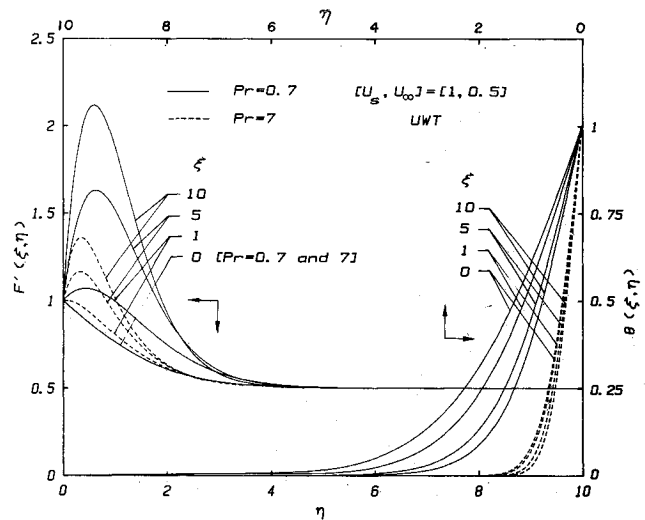


Fig. 8 Velocity and temperature distributions for $(U_s, U_\infty) = (1, 0.5)$, UWT case.

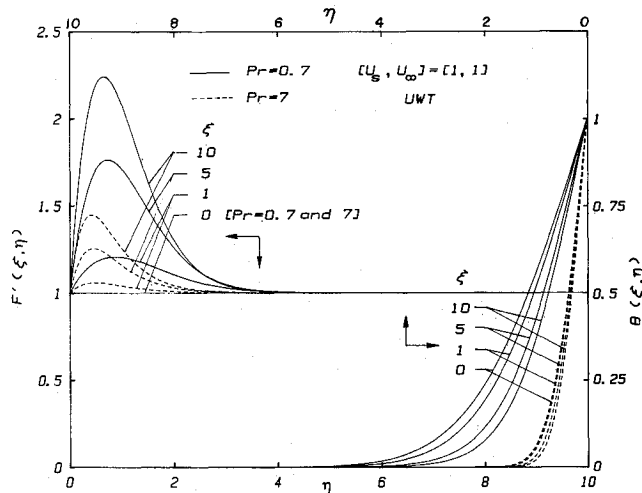


Fig. 7 Velocity and temperature distributions for $(U_s, U_\infty) = (1, 1)$, UWT case.

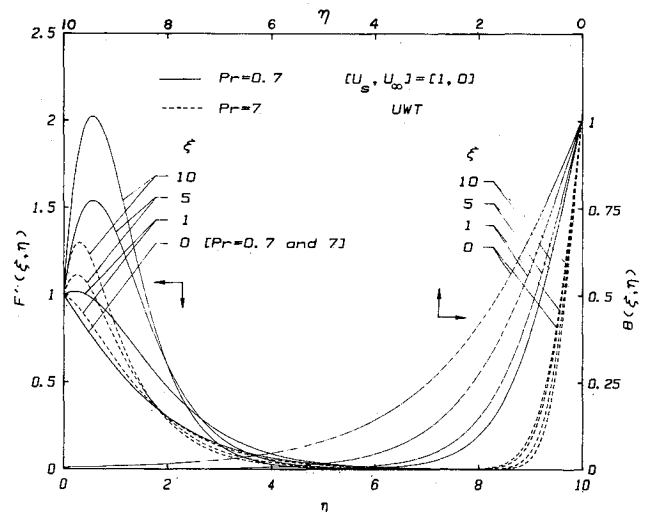


Fig. 9 Velocity and temperature distributions for $(U_s, U_\infty) = (1, 0)$, UWT case.

combinations (U_s, U_∞) of (1,1), (1,0.5), (1,0) and (0.5,1), respectively. In each figure, velocity and temperature profiles are presented only for four typical buoyancy parameter values of 0, 1, 5, and 10. From these figures, it can be seen that both the velocity and temperature distributions are affected by the buoyancy forces, with the velocity field showing a more pronounced effect than the temperature field. Also, significant velocity overshoots occur within the boundary layer as the buoyancy force increases, thus increasing the local wall shear stress. Similarly, an increase in the temperature gradient at the wall with increasing buoyancy force causes an increase in the local heat-transfer rate from the wall. The above-mentioned characteristics displayed by the flow and thermal fields are more subdued for the higher Prandtl number fluid than for the lower Prandtl number fluid. A comparison between the temperature profiles for the velocity combinations $(U_s - U_\infty)$ of (1,0.5) and (0.5,1) (Figs. 8 and 10, respectively) helps to illustrate the heat-transfer characteristics for flows where $|U_s - U_\infty|$ is the same. The steeper temperature gradients shown in Fig. 8 than in Fig. 10 correspond to higher heat-transfer rates in the former case as compared to the latter. This augmented heat-transfer rate when $U_s > U_\infty$ is due to the higher velocity of the fluid particles near the heated sheet,

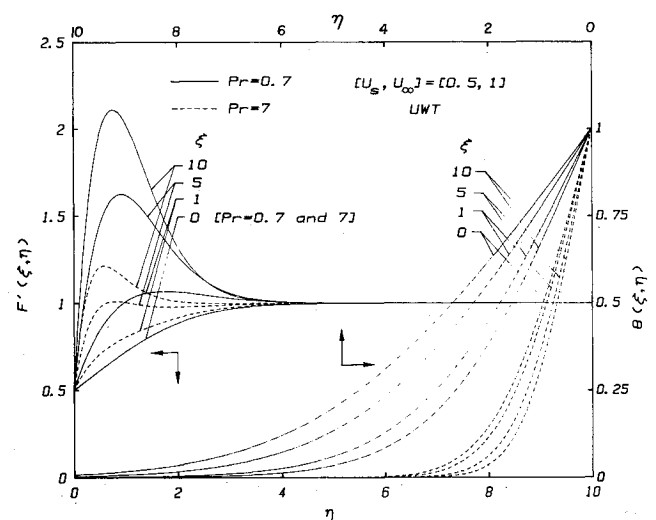


Fig. 10 Velocity and temperature distributions for $(U_s, U_\infty) = (0.5, 1)$, UWT case.

which translates into a higher transport of thermal energy from the surface.

The values of the correlation factor C for the various flowfields and the two heating conditions (UWT and UHF) are listed in Table 1. This table also includes the lower bound a of the buoyancy parameter, above which the mixed convection Nusselt number is more than 5% above the pure forced convection value and the upper bound b , which denotes a 5% departure of the mixed convection Nusselt number from the pure free convection asymptote. Significant errors will result if the asymptotic values of pure forced convection and pure free convection are used in computing the heat-transfer rate in the mixed convection regime.

Conclusion

Mixed convection in laminar boundary layers adjacent to continuous sheets moving in either vertical or inclined directions and subjected to a parallel freestream is analyzed. The thermal buoyancy force significantly alters the thermal and flow fields and hence changes the heat-transfer rate from the surface. Velocity and temperature distributions for various surface/free stream velocity combinations show that the velocity field is affected much more by the buoyancy force than the temperature field. Significant velocity overshoots occur within the boundary layer as the buoyancy force increases, thus causing an increase in the wall shear stress. Similarly, the temperature profiles display a steeper gradient at the wall with the increasing value of the buoyancy parameter, resulting in an increase in the surface heat-transfer rate. The above-mentioned flow and temperature characteristics are presented for Prandtl numbers of 0.7 and 7, with the higher Prandtl number fluid showing a more subdued effect than the lower one. Simple and accurate correlations are presented for calculating the local and average Nusselt numbers for both cases of uniform wall temperature and uniform surface heat flux.

Acknowledgment

The work reported in the paper was supported in part by Grant MEA 83-00785 from the National Science Foundation.

References

- ¹Sakiadis, B.C., "Boundary-Layer Behavior on Continuous Solid Surfaces: II. The Boundary-Layer on a Continuous Flat Surface," *AIChE Journal*, Vol. 7, 1961, pp. 221-225.
- ²Sakiadis, B.C., "Boundary-Layer Behavior on Continuous Solid Surfaces: III. The Boundary-Layer on a Continuous Cylindrical Surface," *AIChE Journal*, Vol. 7, 1961, pp. 467-472.
- ³Moutsoglou, A. and Chen, T.S., "Buoyancy Effects in Boundary Layers on Inclined, Continuous Moving Sheets," *Journal of Heat Transfer*, Vol. 102, 1980, pp. 371-373.
- ⁴Abdelhafez, T.A., "Skin Friction and Heat Transfer on a Continuous Flat Surface Moving in a Parallel Free Stream," *International Journal of Heat and Mass Transfer*, Vol. 28, 1985, pp. 1234-1237.
- ⁵Mucoglu, A. and Chen, T.S., "Mixed Convection on Inclined Surfaces," *Journal of Heat Transfer*, Vol. 101, 1979, pp. 422-426.
- ⁶Chen, T.S., Armaly, B.F., and Aung, W., "Mixed Convection in Laminar Boundary-Layer Flow," *Natural Convection-Fundamentals and Applications*, Hemisphere, New York, 1985, pp. 699-725.
- ⁷Keller, H.B. and Cebeci, T., "Accurate Numerical Methods for Boundary-Layer Flows, I: Two-Dimensional Laminar Flows," *Lecture Notes in Physics: Proceedings of the 2nd International Conference on Numerical Methods in Fluid Dynamics*, Springer-Verlag, New York, Vol. 8, 1971.
- ⁸Keller, H.B. and Cebeci, T., "Accurate Numerical Methods for Boundary-Layer Flows, II: Two-Dimensional Turbulent Flows," *AIChE Journal*, Vol. 10, 1972, pp. 1193-1199.
- ⁹Chen, T.S., Armaly, B.F., and Ramachandran, N., "Correlations for Laminar Mixed Convection Flows on Vertical, Inclined, and Horizontal Flat Plates," *Journal of Heat Transfer*, Vol. 108, 1986, pp. 835-840.
- ¹⁰Armaly, B.F., Chen, T.S., and Ramachandran, N., "Correlations for Laminar Mixed Convection on Vertical, Inclined, and Horizontal Flat Plates with Uniform Surface Heat Flux," *International Journal of Heat and Mass Transfer*, to be published.
- ¹¹Ramachandran, N., Armaly, B.F., and Chen, T.S., "Correlations for Laminar Mixed Convection in Boundary Layers Adjacent to Inclined, Continuous Moving Sheets," *International Journal of Heat and Mass Transfer*, to be published.
- ¹²Churchill, S.W. and Ozoe, H., "Correlation for Laminar Forced Convection in Flow Over an Isothermal Flat Plate and in Developing and Fully Developed Flow in an Isothermal Tube," *Journal of Heat Transfer*, Vol. 95, 1973, pp. 416-419.
- ¹³Ede, A.J., "Advances in Free Convection," *Advances in Heat Transfer*, Vol. 4, Academic Press, New York, 1967, pp. 1-64.
- ¹⁴Fujii, T. and Fujii, M., "The Dependence of Local Nusselt Number on Prandtl Number in the Case of Free Convection Along a Vertical Surface with Uniform Heat Flux," *International Journal of Heat and Mass Transfer*, Vol. 19, 1976, pp. 121-122.